Research Square

Preprints are preliminary reports that have not undergone peer review.
They should not be considered conclusive, used to inform clinical practice,
or referenced by the media as validated information.

Targeting the β-catenin–TCF binding interface for cancer therapy: In silico exploration of Cucumis sativus phytochemicals using Induced-Fit Docking, Molecular Dynamics and ADMET analysis

Samson Marvellous Oladeji
University of Notre Dame
Deborah Ngozi Conteh
Ladoke Akintola University of Technology,
Funmilayo Elizabeth Adeyemi
Babcock University
Timileyin Akinola Akintayo
The Federal University of Technology, Akure
Lukman Abidemi Bello
bellol@purdue.edu
Purdue University West Lafayette
Damilola Comfort Ife-Bolade
Babcock University
Moses Akinwumi Akintunji
The Federal University of Technology, Akure
Festus Slade
University of Warwick
Ridwan Oladimeji Ojo
Federal University of Agriculture

Research Article

Keywords: Wnt/β-catenin signaling pathway, β-catenin-TCF interactions, Cucumis sativus, Molecular docking, Induced-Fit Docking, Molecular Dynamics, ADMET

Posted Date: July 31st, 2025

DOI: https://doi.org/10.21203/rs.3.rs-7048264/v1

License: This work is licensed under a Creative Commons Attribution 4.0 International License. Read Full License

Additional Declarations: No competing interests reported.

Version of Record: A version of this preprint was published at Bulletin of the National Research Centre on August 25th, 2025. See the published version at https://doi.org/10.1186/s42269-025-01354-y.

Abstract

Background

The Wnt/β-catenin signaling pathway plays a vital role in embryogenesis, stem cell regulation, and tissue homeostasis. Aberrant activation of this pathway has been linked to the initiation and progression of various cancers. β-Catenin, a key transcriptional coactivator in this pathway, interacts with T cell factor/Lymphoid enhancer-binding factor (TCF/LEF) transcription factors to drive gene expression critical for oncogenesis. Disrupting this protein–protein interaction (PPI) by directly targeting β-catenin presents a promising therapeutic approach for suppressing oncogenic Wnt signaling. *Cucumis sativus* contains a variety of phytochemicals—such as flavonoids, triterpenoids, and cucurbitacins—known for their anti-inflammatory, antioxidant, and anticancer activities. In this study, computational techniques, including molecular docking and molecular dynamics (MD) simulations, were employed to identify potential β-catenin–TCF interaction inhibitors among bioactive compounds from *C. sativus*. Additionally, absorption, distribution, metabolism, excretion, toxicity (ADMET) predictions were carried out to assess the pharmacokinetic and toxicity profiles of the most promising candidates, offering insights into their potential as lead compounds in anticancer drug development.

Results

The results from binding affinity scores, docking poses, and interaction analyses indicate that Isovitexin-7-O-(6-O-glucosyl)-glucoside (− 9.811 kcal/mol), Cucumerin C (− 8.454 kcal/mol), Kaempferol 3-O-glucoside (− 7.869 kcal/mol), and Kaempferol 3-O-rhamnoside (− 7.738 kcal/mol) are promising inhibitors of the β-catenin–TCF protein–protein interaction. MD simulations showed the stability of the β-catenin–Cucumerin C complex over time. Furthermore, ADMET predictions supported the drug-likeness and favorable pharmacokinetic properties of Cucumerin C, Kaempferol 3-O-rhamnoside, and Isovitexin, highlighting their potential as lead compounds for further anticancer drug development.

Conclusion

This study demonstrates the potential of *C. sativus* phytocompounds as inhibitors of the β-catenin–TCF interaction, suggesting that this plant may serve as a valuable natural source of lead compounds for the development of anticancer agents targeting the Wnt/β-catenin signaling pathway.

Background

Cancer is a major cause of high death rates worldwide. The World Health Organization reported that cancer is accountable for nearly 10 million deaths every year and is the second leading cause of death globally (Johariya et al., 2023). Various factors have been identified as causes of different types of cancer. These factors can be broadly categorized into non-modifiable and modifiable risk factors. Non-modifiable factors include genetics and family history, which cannot be changed. In contrast, modifiable risk factors involve lifestyle choices—such as unhealthy diet, tobacco use, and alcohol consumption—as well as environmental exposures to carcinogens like arsenic, asbestos, cadmium, and benzene (Sobti et al., 2024). Recognizing these risk factors is crucial for creating effective cancer prevention and treatment strategies.

Cancer is defined by the uncontrolled proliferation and spread of abnormal cells. This often results from mutations and dysregulated cellular pathways that promote cell proliferation and survival (M. Zhao et al., 2024). One of the key pathways implicated in many cancers is the Wnt/β-catenin pathway. The Wnt/β-catenin signaling cascade plays a crucial role in embryonic development, tissue regeneration, and cellular homeostasis (J. Liu et al., 2022). The deregulation of Wnt/β-catenin signaling usually leads to various severe diseases, encompassing both cancerous and non-cancerous

conditions. Under normal conditions, the pathway is tightly controlled, aiding in tissue regeneration and stem cell renewal. However, when dysregulated, it becomes oncogenic, contributing to tumor initiation, growth, and metastasis in various cancers, including colorectal, liver, breast, and lung cancers (Samant et al., 2024; H. Zhao et al., 2022).

In Wnt/β-catenin pathway, β-catenin is a central player. In the absence of Wnt signaling, β-catenin levels in the cell are kept low through continuous degradation. However, when the Wnt signaling is activated, it stabilizes β-catenin as it inhibits its phosphorylation by glycogen synthase kinase 3 (GSK-3). As a result, its later degradation via the proteasome is prevented as well, permitting it to build up and move into the nucleus (Fig. 1) (J. Liu et al., 2022). There, β-catenin binds to transcription factors, which results in the activation of genes implicated in cell proliferation, survival, and migration. Activation of these genes is implicated in cancer progression. Given its pivotal role in tumorigenesis, the β-catenin pathway has become a major target for anti-cancer therapies. Researchers are discovering potential mechanisms to stop the unregulated proliferation of cancer cells by focusing on this pathway (Shang et al., 2017; Wang et al., 2022).

Despite considerable advances in oncology, current treatment modalities, including surgery, chemotherapy, and radiotherapy, are often limited by poor selectivity, toxicity, and the emergence of resistance (Amjad et al., 2025; Debela et al., 2021). These shortcomings necessitate the continuous search for safer, more effective therapeutic alternatives. And has led researchers to make findings into the use of natural compounds to create effective and less toxic treatments for cancer (H. Zhang et al., 2023). This research gap necessitates for a computational strategy, utilizing in-silico methods to evaluate and predict the inhibitory potential of compounds. Such approaches enable efficient screening and analysis of phytochemicals against target proteins like β-catenin, facilitating the discovery of promising therapeutic candidates while minimizing experimental expenses and addressing ethical limitations tied to conventional laboratory methods.

Efforts to target β-catenin directly with small-molecule inhibitors have faced significant challenges due to the large and dynamic nature of the β-catenin–TCF interaction interface and the lack of well-defined binding pockets. Nevertheless, recent in silico approaches have demonstrated the feasibility of targeting specific "hot spots" within the β-catenin–TCF PPI interface (Fasolini et al., 2003; Trosset et al., 2006; Voronkov & Krauss, 2013). For instance, Pagare and co-workers identified two key druggable regions on β-catenin using FTMAPS analysis, revealing critical residues such as N430, K435, R469, H470, S473, R474, R515, and N516 that contribute significantly to ligand binding (Pagare et al., 2021). These findings provide a valuable structural framework for the rational design of β-catenin inhibitors.

Phytochemicals, also known as plant secondary metabolites, have been of major interest in the treatment and management of several disease conditions. They include alkaloids, flavonoids, terpenoids, and polyphenols, and been extensively researched for their biological activities. Some of their properties include anti-inflammatory, anti-diabetic, hepatoprotective, antioxidant, and anti-cancer effects (Hilal et al., 2024).

C. sativus (cucumber) is a widely cultivated plant valued not only for its nutritional content but also for its diverse medicinal properties (Fig. 2). Research has identified several phytochemicals within *C. sativus*, including flavonoids, triterpenoids, and cucurbitacin, which exhibit diverse bioactivities such as anti-inflammatory, antioxidant, and anticancer properties (Tuama & Mohammed, 2019). In particular, cucurbitacins have shown promise as inhibitors of the β-catenin pathway, positioning C. sativus as a potential source of β-catenin inhibitors (Dandawate et al., 2020; Feng et al., 2014). Despite the known efficacy of various natural products in inhibiting β-catenin, there is a lack of comprehensive in silico studies specifically focusing on phytochemicals from *C. sativus*. Given the promising bioactivities observed in *C. sativus* phytochemicals, this study evaluated the inhibitory potential of phytochemicals derived from *C. sativus* against β-catenin using a comprehensive in silico approach. By targeting validated hot spots within the β-catenin–TCF interface, that may serve as effective and selective therapeutic agents for cancer treatment. The exploration of *C. sativus* aligns with the increasing focus on natural products for cancer therapy.

Methods

Ligand selection and preparation

Phytochemicals reported from *C. sativus* were obtained in standard data format (SDF) from the PubChem online database (Bauleth et al., 2025; Mukherjee et al., 2013). For compounds not available in the database, chemical structures were manually drawn using ChemDraw. All ligands used in the molecular docking studies were prepared using the LigPrep tool from the Schrödinger Suite (version 2020-3). The OPLS4 force field was utilized to simulate atomic interactions within the system. To reflect physiological conditions, the ionization states of the ligands were determined at pH 7.2 ± 0.2, ensuring accurate low-energy three-dimensional structures and proper stereochemistry. Additionally, stereoisomers were generated while maintaining the ligands' original chiral centers.

β-Catenin ligand binding site selection

Potential ligand-binding sites on the surface of β-catenin have been identified using various computational approaches. One such method is the Putative Active Site with Spheres (PASS) program, which was initially applied to the β-catenin/TCF3 crystal structure and later validated with the β-catenin/TCF4 complex (Graham et al., 2000; Poy et al., 2001). PASS identifies binding pockets by placing a grid of probe spheres across the protein surface and assessing geometric and physicochemical features such as pocket depth, volume, and hydrophobicity. These concave regions, likely to accommodate small molecules, are scored based on size, shape, and enclosure to evaluate their suitability as potential binding sites for virtual screening or drug design. To further validate the regions identified by PASS, a more rigorous approach using solvent-accessible surface calculations via the FLO_QXP package has also been employed (Trosset et al., 2006).

Another study utilized FTMAP to evaluate the druggability of the β-catenin–TCF protein–protein interaction (PPI) interface (Pagare et al., 2021). FTMAP probes billions of positions using small organic molecules and determines their favorable binding poses based on empirical free energy calculations. It clusters these poses and ranks them, identifying protein regions that bind multiple probe clusters as potential "hot spots" for small-molecule intervention. In this study, to identify druggable hot spots on β-catenin, a consensus region was determined around residues ARG469 and ARG515. This region, rich in charged residues, is capable of engaging in both hydrogen bonding and hydrophobic interactions. Targeting these residues may effectively disrupt the β-catenin–TCF interaction, offering a promising strategy for inhibiting this oncogenic PPI.

Protein preparation

Preparation of protein was carried out as previously described (Oladeji et al., 2025). The crystal structure of β-catenin (PDB ID: 1JDH) was retrieved from the Protein Data Bank. Using the Protein Preparation Wizard in Glide (Schrödinger Suite 2020-3), hydrogen atoms were added, bond orders were corrected, and disulfide bonds were established. Missing loops and side chains were reconstructed with Prime 3.3. Water molecules located more than 3.0 Å from any heteroatoms were deleted. The structure was then energy-minimized using the OPLS4 force field and the protonation states were optimized with PROPKA (Søndergaard et al., 2011).

Induced Fit Docking (IFD)

The interactions between β-catenin and the ligands were evaluated using the Induced Fit Docking (IFD) protocol in Schrödinger Maestro 12.5. This method accommodates substantial conformational changes in the receptor upon ligand binding, thereby enhancing the accuracy of ligand placement. The binding site was defined as a 16 Å region centered around the ARG469 residue to focus the docking process on β-catenin identified hot spot.

Molecular Dynamics (MD) Simulations

MD simulations were performed on the protein–ligand complexes using Desmond 2.0, a simulation tool developed by Schrödinger LLC, New York, NY, USA. Each simulation was carried out for 100 nanoseconds. System setup was completed using the 'System Builder' module in Maestro, employing the TIP3P water model within an orthorhombic simulation box measuring 10 × 10 × 10 Å. To ensure charge neutrality, counterions (Cl^-) were added. The simulations utilized the OPLS4 force field and RESPA integrator settings. Prior to initiating the MD runs, all systems underwent energy minimization and equilibration. Simulations were conducted under the NPT ensemble, maintaining a constant temperature of 310 K and a pressure of 1 atm. Trajectory data were saved every 100 picoseconds for post-simulation analysis, and system stability was assessed by tracking the root-mean-square deviation (RMSD) of both the protein and ligand throughout the simulation period.

ADMET Prediction

The pharmacokinetic and toxicological profiles (ADMET) of the test compounds were assessed using predictive tools provided by the SwissADME and PROTOX-3 online platforms (Banerjee et al., 2024; Daina et al., 2017). This analysis included computational predictions of the ligands' absorption, distribution, metabolism, excretion, and toxicity characteristics.

Results and discussion

Induced-Fit Docking (IFD)

For this study, seven known inhibitors of β-catenin (iCRT3, apigenin, PKF118-744, PKF115-584, PKF118-310, PNU-74654, and silibinin) were used as standards. The selection of these standards was guided by their diverse chemical structures, experimentally confirmed interaction with β-catenin at the TCF binding region, and previously reported evidence of their inhibitory activity or binding affinity in published studies (Abdolmaleki & Ghasemi, 2016; M. Yan et al., 2017). These standards were docked into the previously identified binding sites (see Methodology) of β-catenin (PDB: 1JDH) using the Schrödinger's IFD docking protocol. After the docking validations with the known standards, 45 phytochemicals from *C. sativus* were screened.

IFD method addresses the challenge of predicting how a ligand fits into a protein's active site, especially when the site changes shape upon binding (Sherman, Beard, et al., 2006). Traditional experimental techniques like X-ray crystallography are often time-consuming or impractical, but IFD uses two computational tools—Glide and Prime—to simulate this process efficiently (Fig. 3). It begins by docking the ligand into the protein using flexible settings that allow for diverse binding poses, temporarily adjusting highly flexible regions if needed. Prime then refines the protein structure by repositioning nearby side chains to better fit the ligand, followed by energy minimization. Finally, the ligand is redocked into the adjusted protein structure, and each resulting complex is evaluated and scored based on how well the ligand fits and the overall stability of the interaction (Sherman, Day, et al., 2006).

Table 1
IFD docking scores of standard ligands and phytochemicals from Cucumber

Standards	Docking score (kcal/mol)	Ligands	Docking score (kcal/mol)
Apigenin	-7.375	Indole-3-carboxylic acid	-6.799
PKF118-310	-6.229	Isoorientin	-6.737
PKF115-584	-5.624	Isovitexin-7,2" -di-O-glucoside	-6.607
iCRT3	-5.442	Isovitexin 4' ,2"-di-O-glucoside	-6.334
PKF118-744	-4.986	Cucurbitacin E	-6.189
PNU-74654	-3.986	Quercetin 3-O-glucoside	-6.165
Silibinin	-2.228	Cucumerin A	-6.084
Ligands		Isovitexin-7-O-(6"-O-glucosyl)-glucoside	-6.079
Isovitexin-7-O-(6-O-glucosyl)-glucoside	-9.811	Kaempferol 3-O-rhamnoside	-6.049
Cucumerin C	-8.454	Isovitexin-2"-O-(6""-O-p-coumaroyl) glucoside	-5.719
Kaempferol 3-O-glucoside	-7.869	Cucurbitacin I	-5.688
Kaempferol 3-O-rhamnoside	-7.738	Cucurbitacin D	-5.687
Isovitexin-2-O-(6-O-p-coumaroyl)-glucoside	-7.715	Cucumerin A	-5.667
Isovitexin	-7.714	Isovitexin-2"-O-glucoside-6"-O-p-coumarate	-5.555
Cucumerin D	-7.22	Cucumerin B	-5.517
Isorhamnetin-3-O-glucoside	-7.214	Cucumegastigmane I	-5.121
Apigenin 7-O-(6"-O-feruloyl)glucoside	-7.176	Dehydrovomifoliol	-4.974
Isovitexin-2-O-(6-O-feruloyl)-glucoside	-7.135	Indole-3-aldehyde	-4.876
Apigenin 7-O-(6"-O-p-coumaroyl) glucoside	-7.036	Cucurbitacin B	-4.83
Isovitexin-2"-O-glucoside	-6.972	Vicenin 2	-4.682
Cucumegastigmane II	-6.951	Quercetin 3-O-glucoside	-4.549
Orientin	-6.91	Isovitexin-4,2-O-glucoside	-4.281
Vitexin	-6.803	Cucubitacin A	-4.26
Cucumerin A	-4.219	Cucumerin A	-4.219
Quercetin 3-O-glucoside	-4.181	Quercetin 3-O-glucoside	-4.181
Cucurbitacin	-4.065	Cucurbitacin	-4.065
Cucumerin B	-4		

The molecular docking results show that Apigenin has the lowest docking score among the standards docked (-7.375 kcal/mol), followed by PKF118-310 (-6.229 kcal/mol), PKF115-584 (-5.624 kcal/mol), iCRT3 (-5.442 kcal/mol), PKF118-744 (-4.986 kcal/mol), and PNU-74654 (-3.986 kcal/mol), with Silibinin exhibiting the highest docking score (Table 1). Since lower docking scores typically indicate stronger binding affinity and greater inhibitory potential, these results suggest that Apigenin may serve as a particularly effective inhibitor of β-catenin–TCF interactions. Apigenin is a naturally occurring flavonoid abundant in various fruits and vegetables (Zhou et al., 2017). It is well known for its potent anticancer and anti-inflammatory properties, along with a favorable safety profile in biological systems (Naponelli et al., 2024; X. Yan et al., 2017). Apigenin has been shown to disrupt multiple cancer-related signaling pathways and inhibit the proliferation of diverse human cancer cell lines, including those originated from leukemia, breast, colon, lung, skin, thyroid, and prostate cancers (Xu et al., 2016; X. Yan et al., 2017). Shukla and co-workers demonstrated that Apigenin inhibits the β-catenin–TCF interaction in DU145 prostate cancer cells, prevents β-catenin nuclear translocation, and downregulates oncogenic targets such as c-Myc and cyclin D1 (Shukla et al., 2007). In TRAMP mice, Apigenin similarly suppressed prostate tumor progression by targeting β-catenin signaling (Shukla et al., 2007).

PKF118-310, PKF115-584, and PKF118-744 were previously identified through high-throughput screening (HTS) of 7,000 natural compounds using an ELISA-based assay, and have reported IC_{50} values of 0.8 μM, 3.2 μM, and 2.4 μM, respectively (Lepourcelet et al., 2004). The trend observed in our docking results is consistent with these experimental data, particularly the superior performance of PKF118-310, thereby further supporting the predictive accuracy and reliability of our IFD protocol.

PNU-74654 was identified as a promising candidate in the first study to target hotspot regions of β-catenin, conducted by Trosset and co-workers (Trosset et al., 2006). In this study, approximately 17,700 compounds were screened using a combination of in silico docking and biophysical screening to identify molecules that could disrupt the β-catenin–TCF PPI, specifically targeting the LYS435 and ARG469 hotspot regions. In a separate study, Gonsalves and co-workers employed RNA interference to suppress AXIN expression and combined this approach with integrated screening techniques (Gonsalves et al., 2011). This strategy led to the discovery of iCRT3, a small molecule that effectively inhibited catenin-responsive transcription (CRT).

Despite the known biological activity of Apigenin, detailed molecular interaction data between Apigenin and β-catenin have not been reported until now (Naponelli et al., 2024; Shukla et al., 2007). As shown in Fig. 4, Apigenin forms multiple hydrogen bonds with key residues on β-catenin, including LYS435, SER473, ARG515, and VAL511. The phenolic ring of Apigenin occupies the large positively charged region of β-catenin, while the benzene diol moiety aligns with the polar region. Since the positively charged surface of β-catenin is critical for its interaction with TCF, Apigenin's binding to this region likely disrupts the β-catenin–TCF PPI, providing a molecular basis for its observed inhibitory activity (Fasolini et al., 2003).

Similarly, PKF118-310, PKF115-584, and iCRT3 primarily occupy the positively charged region of β-catenin. Both PKF115-584 and iCRT3 form hydrogen bonds with the negatively charged GLU571 residue. In addition, PKF115-584 interacts with CYS429 and ASN516, while iCRT3 forms a hydrogen bond with ARG474. PNU-74654 which was originally identified via in-silico docking, also hydrogen bond with ASN516 and forms a π-cation interaction with ARG515. Notably, ASN516, ARG515 and ARG474 have also been highlighted by other molecular docking studies as key residues involved in β-catenin inhibition (Pagare et al., 2021; Tian et al., 2012; Yu et al., 2013).

Phytochemicals IFD Analysis

Forty-five (45) phytochemicals isolated from Cucumber were screened which belong to three major different natural products categories, Flavonoids, Cucumerinoids and Curcubitacins (Bauleth et al., 2025; Mukherjee et al., 2013). Six of these phytochemicals namely, Isovitexin-7-O-(6-O-glucosyl)-glucoside (-9.811), Cucumerin C (-8.454), Kaempferol 3-O-

glucoside (-7.869), Kaempferol 3-O-rhamnoside (-7.738), Isovitexin-2-O-(6-O-p-coumaroyl)-glucoside (-7.715) and Isovitexin (-7.714) have shown docking scores better than Apigenin (Table 1).

Molecular interaction analysis of the top four ligands reveals that they predominantly occupy the positively charged region of β-catenin, which may effectively disrupt the β-catenin–TCF protein–protein interaction (Fig. 5). Notably, all four ligands interact with ARG469, either through hydrogen bonding or π-cation interactions. ARG469 is a key polar residue known to play a critical role in β-catenin's interaction with TCF4 (Trosset et al., 2006). In addition to ARG469, other identified essential polar residues involved in TCF binding include ARG515, LYS435, LYS508, and GLU571 (Fasolini et al., 2003; Pagare et al., 2021; Trosset et al., 2006). Each of the top four ligands forms interactions with at least three of these critical residues, further supporting their potential to inhibit β-catenin–TCF complex formation and downstream signaling.

The top four ranked ligands all contain the apigenin core structure (Fig. 6), which is not surprising, as apigenin itself was among the highest-ranking β-catenin inhibitors used as standards in this study. Apigenin core structure plays a significant therapeutic role due to its well-documented bioactivity, particularly its anti-cancer potential and its relatively low toxicity (Naponelli et al., 2024; Xu et al., 2016). As a naturally occurring flavonoid, apigenin has been demonstrated to influence important signaling pathways that play a role in tumor progression, including the Wnt/β-catenin pathway (Xu et al., 2016; X. Yan et al., 2017). Its planar aromatic structure facilitates π-π stacking and hydrogen bonding interactions within the β-catenin binding pocket, making it an ideal scaffold for designing PPI inhibitors. Moreover, derivatives of apigenin have been shown to enhance potency and specificity for targeted cancer therapy, supporting its value as a lead framework (R. Liu et al., 2013; S. Liu et al., 2024). However, due to apigenin's limitations on absorption and bioavailability, analogs or derivatives of apigenin are desirable to enhance the oral bioavailability.

Molecular Dynamics (MD) Simulations

To evaluate the stability of the ligand–protein interactions, MD simulations were conducted on the two top-ranked ligands: Isovitexin-7-O-(6-O-glucosyl)-glucoside (–9.811) and Cucumerin C (–8.454). MD simulations provide dynamic perspective on molecular behavior by modeling the motion of atoms and molecules over time under controlled temperature and pressure conditions. Unlike docking, which offers a static snapshot, MD allows for the assessment of complex stability, conformational changes, and key molecular interactions in a more realistic, time-evolving environment. This approach is crucial for validating docking results and gaining deeper insights into the binding affinity and structural integrity of the ligand–protein complex under near-physiological conditions.

To interpret the outcomes of the simulations, key parameters such as Root Mean Square Deviation (RMSD), Root Mean Square Fluctuation (RMSF), and protein–ligand contact analyses were employed. These metrics provide insight into the structural stability, flexibility, and interaction patterns of the ligand–protein complexes throughout the simulation period.

RMSD analysis is a key metric in molecular dynamics simulations for assessing structural stability and conformational changes (Sargsyan et al., 2017). For proteins, RMSD is typically calculated by aligning all frames to a reference structure based on the backbone atoms, providing insight into how much the structure deviates over time. Small fluctuations (generally within 1–3 Å) are common for compact, globular proteins and suggest the system is near equilibrium (Coutsias & Wester, 2019). However, persistent drifts or large deviations may indicate significant conformational rearrangements or insufficient simulation time for equilibration. Ligand RMSD, often computed after aligning the complex on the protein backbone, tracks the positional stability of the ligand within the binding pocket. A ligand RMSD that significantly exceeds that of the protein may signal detachment or diffusion away from the active site, highlighting potential instability in the binding interaction.

The RMSD plots of β-catenin in complex with Isovitexin-7-O-(6-O-glucosyl)-glucoside and Cucumerin C exhibit values ranging from 0.5 to 4.5 Å (Fig. 7). While these values are slightly higher than the typical range for small, globular proteins,

the protein RMSD in both complexes shows minimal initial fluctuation followed by stabilization, indicating that the systems have reached equilibrium. A similar trend is observed in the ligand RMSD profiles, although the β-catenin complex with Isovitexin-7-O-(6-O-glucosyl)-glucoside displays more pronounced fluctuations at the start of the simulation, suggesting greater initial mobility within the binding site.

The RMSF values reflect the local flexibility of each amino acid residue in the protein backbone, as shown in Fig. 8. The RMSF profiles for both Isovitexin-7-O-(6-O-glucosyl)-glucoside and Cucumerin C displayed nearly identical fluctuation patterns throughout the simulation, with values generally remaining within 3.0 Å. An exception was observed around residue 400, where a peak in fluctuation suggests increased flexibility in that region. Green vertical bars in the plot highlight protein residues that interact with the ligand. The ligand RMSF, represented by the red line, illustrates atomic-level fluctuations. Notably, Isovitexin-7-O-(6-O-glucosyl)-glucoside exhibited greater fluctuation compared to Cucumerin C, indicating a higher degree of movement within the binding site.

Protein–ligand interactions can be effectively monitored throughout the course of a molecular dynamics simulation, providing insights into the stability and nature of the binding. These interactions are typically categorized into four types: hydrogen bonding, hydrophobic interactions, ionic (electrostatic) interactions, and water-mediated bridges. As shown in Fig. 9, the protein–ligand contacts demonstrated significant hydrogen bonding activity. The stacked bar charts in the figure are normalized over the trajectory, meaning that a value of 0.7 indicates the interaction was maintained for 70% of the simulation time. Values greater than 1.0 are possible when a single residue forms multiple contacts of the same type with the ligand. For Isovitexin-7-O-(6-O-glucosyl)-glucoside, residues GLU571 (2.0), GLU568 (0.8), and GLU469 (0.9) showed the most frequent hydrogen bonding throughout the simulation. Similarly, for Cucumerin C, ARG469 (1.0), GLU568 (0.8), and LYS435 (0.7) exhibited the highest hydrogen bond occupancy. In addition, Fig. 9 includes a schematic representation of ligand atom interactions with protein residues that occurred for more than 30% of the simulation time. For Isovitexin-7-O-(6-O-glucosyl)-glucoside, notable hydrogen bonds were observed with GLU571 (71%), ARG469 (58%), GLU568 (38%), and ARG515 (41%). Cucumerin C interacted primarily with ARG469 (97%), GLU568 (84%), LYS435 (70%), LYS508 (48%), CYS429 (40%), and ARG515 (34%). It is important to note that GLU571 formed multiple hydrogen bonds with different hydroxyl groups on Isovitexin-7-O-(6-O-glucosyl)-glucoside, although only the interaction with the highest contact frequency is reported here. Notably, previous studies have identified many of these residues as key components of the β-catenin–TCF protein–protein interaction interface (Fasolini et al., 2003; Pagare et al., 2021; M. Yan et al., 2017).

ADMET property prediction

ADMET (absorption, distribution, metabolism, excretion, and toxicity) analysis plays a crucial role in the process of drug discovery. It offers a cost-effective in silico approach to predict how a drug will behave within a biological system, helping to assess its efficacy and safety early in development (van de Waterbeemd & Gifford, 2003). In this study, we use the SwissADME and Protox-3 servers to predict the drug-like and toxicity profile of the top ten lead compounds and standard compounds.

The hydrophilicity of phytochemicals is commonly assessed using the log P value, which reflects the compound's partitioning between n-octanol and water. For optimal drug-likeness, a log P value is generally expected to fall within the range of 0 to 5 (Mannhold et al., 2009). Compounds with log P values above 5 are considered excessively lipophilic, while those below 1 are deemed too hydrophilic. Among the standard compounds analyzed, only PKF118-310 (-0.41) and PKF115-584 (5.95) fall outside this optimal range, yet both remain potentially orally bioavailable (Table 2). Regarding the ligands, among the top 10, only Cucumerin C (0.49), Kaempferol 3-O-rhamnoside (0.67), Isorhamnetin-3-O-glucoside (0.12), and Apigenin 7-O-(6-O-feruloyl)glucoside (1.88) exhibit log P values within the ideal range for oral bioavailability. Additionally, all the standard compounds comply with Lipinski's rule of five, except PKF115-584, which violates two criteria (Jia et al., 2020). In contrast, all the ligands exceed one violation, primarily due to high molecular weights (greater than 500 Da), low log P values, and more than five hydrogen bond donors. Nonetheless, it is worth noting that several

FDA-approved drugs exceed these thresholds, particularly in terms of molecular weight and hydrogen bonding capacity (Roskoski, 2023). A detailed summary of the predicted physicochemical properties is presented in Table 2.

Table 3 presents a summary of the pharmacokinetic characteristics of the standard compounds and ligands. A key parameter assessed is gastrointestinal (GI) absorption, where all ligands demonstrate relatively low absorption compared to the standards. This suggests that, for oral administration, strategies such as formulation optimization or the use of absorption enhancers may be required to improve bioavailability. Alternatively, if non-oral delivery routes (such as intravenous administration) are considered, low GI absorption may pose less of a challenge. Most of the ligands are predicted to be P-glycoprotein (P-gp) substrates, with the exceptions being Kaempferol 3-O-rhamnoside, Isovitexin, and Apigenin 7-O-(6-O-feruloyl)glucoside. P-gp, a member of the ATP-binding cassette (ABC) transporter family, plays a critical role in effluxing xenobiotics from cells, thereby limiting intracellular drug accumulation and therapeutic efficacy. Furthermore, neither the standards nor the ligands are predicted to cross the blood–brain barrier, except for PNU-74654. Cytochrome P450 (CYP) enzymes, which are central to phase I drug metabolism, are also evaluated to assess potential drug–drug interaction risks. While several of the standard compounds are predicted to inhibit CYP isoforms, all of the ligands are expected to be non-inhibitors, suggesting a lower likelihood of CYP-mediated drug–drug interactions.

Table 2
Physicochemical properties of the standards and the top 10 ligands.

Compound	Mol MW (g/mol)	Consensus log P	ESOL log S	ESOL class	Bioavailability score	Rule of five
Apigenin	270.24	2.11	-3.94	Soluble	0.55	0
PKF118-310	193.16	-0.41	-1.15	Very soluble	0.55	0
PKF115-584	790.76	5.95	-9.50	Poorly soluble	0.11	2
iCRT3	394.53	4.52	-5.21	Moderately soluble	0.55	0
PKF118-744	324.33	2.96	-4.47	Moderately soluble	0.55	0
PNU-74654	320.34	3.52	-4.58	Moderately soluble	0.55	0
Silibinin	482.44	1.59	-4.14	Moderately soluble	0.55	0
Isovitexin-7-O-(6-O-glucosyl)-glucoside	756.66	-3.45	-1.80	Very soluble	0.17	3
Cucumerin C	712.69	0.49	-4.74	Moderately soluble	0.17	3
Kaempferol 3-O-glucoside	448.38	-0.09	-3.18	Soluble	0.17	2
Kaempferol 3-O-rhamnoside	432.38	0.67	-3.47	Soluble	0.55	1
Isovitexin-2-O-(6-O-p-coumaroyl)-glucoside	740.66	-0.36	-4.31	Moderately soluble	0.17	3
Isovitexin	432.38	-0.02	-2.84	Soluble	0.55	1
Cucumerin D	714.67	-0.08	-4.38	Moderately soluble	0.17	3
Isorhamnetin-3-O-glucoside	478.40	0.12	-3.26	Soluble	0.17	2
Apigenin 7-O-(6-O-feruloyl)glucoside	608.55	1.88	-5.62	Moderately soluble	0.17	3
Isovitexin-2-O-(6-O-feruloyl)-glucoside	770.69	-0.25	-4.40	Moderately soluble	0.17	3

Table 3
Pharmacokinetic properties of the standards and the top 10 ligands.

Compound	GI absorption	BBB permeant	Pgp substrate	CYP1A2 inhibitor	CYP2C19 inhibitor	CYP2C9 inhibitor	CYP2D6 inhibitor	CYP3A4 inhibitor
Apigenin	High	No	No	Yes	No	No	Yes	Yes
PKF118-310	High	No	No	No	No	No	No	No
PKF115-584	Low	No	Yes	No	No	Yes	No	No
iCRT3	High	No	No	Yes	Yes	Yes	Yes	Yes
PKF118-744	High	No	No	Yes	No	Yes	No	Yes
PNU-74654	High	Yes	No	Yes	Yes	Yes	Yes	No
Silibinin	Low	No	No	No	No	No	No	Yes
Isovitexin-7-O-(6-O-glucosyl)-glucoside	Low	No	Yes	No	No	No	No	No
Cucumerin C	Low	No	Yes	No	No	No	No	No
Kaempferol 3-O-glucoside	Low	No	No	No	No	No	No	No
Kaempferol 3-O-rhamnoside	Low	No	Yes	No	No	No	No	No
Isovitexin-2-O-(6-O-p-coumaroyl)-glucoside	Low	No	Yes	No	No	No	No	No
Isovitexin	Low	No	No	No	No	No	No	No
Cucumerin D	ow	No	Yes	No	No	No	No	No
Isorhamnetin-3-O-glucoside	Low	No	Yes	No	No	No	No	No
Apigenin 7-O-(6-O-feruloyl)glucoside	Low	No	No	No	No	Yes	No	No
Isovitexin-2-O-(6-O-feruloyl)-glucoside	Low	No	Yes	No	No	No	No	No

Table 4 presents the predicted toxicity profiles of the standard compounds and ligands as estimated by the ProTox-II online server, focusing on LD_{50} values (mg/kg), toxicity classification, and key toxicological endpoints such as hepatotoxicity and carcinogenicity. All compounds, both standards and ligands, fall within toxicity classes 4 and 5, indicating moderate toxicity, with LD_{50} values ranging from 500 to 5000 mg/kg. An exception is PKF118-310, which is classified as toxicity class 2, suggesting it may be fatal if swallowed. Overall, the compounds are predicted to be non-carcinogenic and non-hepatotoxic, with the exception of the standard PNU-74654, which shows potential for both hepatotoxicity and carcinogenicity.

Table 4
Protox 3 toxicity profiles of the standards and the top 10 ligands.

Compound	Predicted LD50 (mg/kg)	Predicted toxicity class	Carcinogenicity	Hepatotoxicity
Apigenin	2500	5	Inactive	Inactive
PKF118-310	8	2	Inactive	Inactive
PKF115-584	500	4	Inactive	Inactive
iCRT3	1000	4	Inactive	Inactive
PKF118-744	1000	4	Inactive	Inactive
PNU-74654	1000	4	Active	Active
Silibinin	2000	4	Inactive	Inactive
Isovitexin-7-O-(6-O-glucosyl)-glucoside	5000	5	Inactive	Inactive
Cucumerin C	536	4	Inactive	Inactive
Kaempferol 3-O-glucoside	5000	5	Inactive	Inactive
Kaempferol 3-O- rhamnoside	5000	5	Inactive	Active
Isovitexin-2-O-(6-O-p-coumaroyl)-glucoside	5000	5	Inactive	Inactive
Isovitexin	159	3	Inactive	Inactive
Cucumerin D	5000	5	Inactive	Inactive
Isorhamnetin-3-O-glucoside	5000	5	Inactive	Inactive
Apigenin 7-O-(6-O-feruloyl)glucoside	5000	5	Inactive	Inactive
Isovitexin-2-O-(6-O-feruloyl)-glucoside	1000	4	Inactive	Inactive

Conclusions

Designing small molecules to disrupt PPIs remains a significant challenge in drug discovery. In this study, a computational approach was employed to identify four promising phytoconstituents from *C. sativus*—Isovitexin-7-O-(6-O-glucosyl)-glucoside, Cucumerin C, Kaempferol 3-O-glucoside, and Kaempferol 3-O-rhamnoside—as potential inhibitors of the β-catenin–TCF interaction, outperforming standard reference compounds in docking evaluations. Among these, Cucumerin C demonstrated notable stability in molecular dynamics simulations when bound to β-catenin. ADMET profiling further revealed favorable drug-like characteristics for Cucumerin C, Kaempferol 3-O-rhamnoside, and Isovitexin, including acceptable physicochemical and pharmacokinetic properties. These findings suggest that *Cucumis sativus* may be a promising natural source of drug-like compounds capable of suppressing tumor growth by targeting β-catenin within the Wnt/β-catenin signaling pathway. Further lead optimization and comprehensive in vitro and in vivo validation are recommended to support these computational predictions.

Abbreviations

IFD: Induced-fit docking; ADMET: Absorption, distribution, metabolism, excretion, toxicity; RMSD: Root-mean-square deviation; RMSF: Root-mean-square fluctuation; TCF/ LEF: T cell factor/Lymphoid enhancer-binding factor; GSK-3: glycogen synthase kinase 3; PASS; Putative Active Site with Spheres; PPI: Protein–protein interaction; CYP: Cytochrome p450; FDA: Food and Drug Administration. LD_{50}: Lethal Dose 50%.

Declarations

Acknowledgments

This research has no acknowledgment.

Authors' contributions

Conceptualization, SMO; methodology, SMO, DNC, TAA, MAA, DCI; software, SMO; validation, SMO; formal analysis, SMO and DNC; investigation, SMO. and LAB.; resources, SMO, FEA; data curation, SMO, DNC, TAA, FS, ROO; writing—original draft preparation, SMO, ROO, FS; writing—review and editing, SMO., FEA, DCI, and LAB; visualization, SMO; supervision, SMO and LAB; project administration, SMO.

Competing interests

No competing interest.

Funding

This research was conducted without the support of external funding.

Consent for publication

Not applicable.

Availability of data and materials

Data available on request.

Ethical approval and consent to participate

Not applicable.

Author details

[1]Chemistry Department, Purdue University, West Lafayette, IN 47907, USA.

[2]Department of Chemistry and Biochemistry, University of Notre Dame, Notre Dame, IN 46556, USA

[3]Ladoke Akintola University of Technology, Teaching Hospital, Ogbomoso, Nigeria.

[4]Department of Biochemistry, School of Basic Medical Sciences, Babcock University Ilishan-Remo, Ogun State, Nigeria.

[5]Department of Chemistry, Federal University of Technology Akure, Akure, Ondo State, Nigeria.

[6]University of Warwick, Department of Chemistry, Coventry, United Kingdom

[7]Federal University of Agriculture, Abeokuta, Ogun State, Nigeria

References

1. Abdolmaleki, A., & Ghasemi, J. B. (2016). Dual-acting of Hybrid Compounds—A New Dawn in the Discovery of Multi-target Drugs: Lead Generation Approaches. *Current Topics in Medicinal Chemistry*, *17*(32), Article 32. https://doi.org/10.2174/1568026616666160927151144
2. Amjad, M. T., Chidharla, A., & Kasi, A. (2025). Cancer Chemotherapy. In *StatPearls*. StatPearls Publishing. http://www.ncbi.nlm.nih.gov/books/NBK564367/
3. Banerjee, P., Kemmler, E., Dunkel, M., & Preissner, R. (2024). ProTox 3.0: A webserver for the prediction of toxicity of chemicals. *Nucleic Acids Research*, *52*(W1), W513–W520. https://doi.org/10.1093/nar/gkae303
4. Bauleth, M. Z., Sheehama, J., Cheikhyoussef, N., Cheikhyoussef, A., Makhaba, M., Sharma, R., Cupido, C. N., & Hussein, A. A. (2025). Correction to: Phytochemicals from Cucumber (Cucumis sativus) By-products. In M. F. Ramadan (Ed.), *Bioactive Phytochemicals in By-products from Bulb, Flower and Fruit Vegetables* (pp. C1–C1). Springer Nature Switzerland. https://doi.org/10.1007/978-3-031-77399-0_14
5. Coutsias, E. A., & Wester, M. J. (2019). RMSD and Symmetry. *Journal of Computational Chemistry*, *40*(15), 1496–1508. https://doi.org/10.1002/jcc.25802
6. Daina, A., Michielin, O., & Zoete, V. (2017). SwissADME: A free web tool to evaluate pharmacokinetics, drug-likeness and medicinal chemistry friendliness of small molecules. *Scientific Reports*, *7*(1), 42717. https://doi.org/10.1038/srep42717
7. Dandawate, P., Subramaniam, D., Panovich, P., Standing, D., Krishnamachary, B., Kaushik, G., Thomas, S. M., Dhar, A., Weir, S. J., Jensen, R. A., & Anant, S. (2020). Cucurbitacin B and I inhibits colon cancer growth by targeting the Notch signaling pathway. *Scientific Reports*, *10*(1), 1290. https://doi.org/10.1038/s41598-020-57940-9
8. Debela, D. T., Muzazu, S. G., Heraro, K. D., Ndalama, M. T., Mesele, B. W., Haile, D. C., Kitui, S. K., & Manyazewal, T. (2021). New approaches and procedures for cancer treatment: Current perspectives. *SAGE Open Medicine*, *9*, 20503121211034366. https://doi.org/10.1177/20503121211034366
9. Fasolini, M., Wu, X., Flocco, M., Trosset, J.-Y., Oppermann, U., & Knapp, S. (2003). Hot Spots in Tcf4 for the Interaction with β-Catenin *. *Journal of Biological Chemistry*, *278*(23), 21092–21098. https://doi.org/10.1074/jbc.M301781200
10. Feng, H., Zang, L., Zhao, Z.-X., & Kan, Q.-C. (2014). Cucurbitacin-E Inhibits Multiple Cancer Cells Proliferation Through Attenuation of Wnt/β-Catenin Signaling. *Cancer Biotherapy and Radiopharmaceuticals*, *29*(5), 210–214. https://doi.org/10.1089/cbr.2014.1614
11. Gonsalves, F. C., Klein, K., Carson, B. B., Katz, S., Ekas, L. A., Evans, S., Nagourney, R., Cardozo, T., Brown, A. M. C., & DasGupta, R. (2011). An RNAi-based chemical genetic screen identifies three small-molecule inhibitors of the Wnt/wingless signaling pathway. *Proceedings of the National Academy of Sciences of the United States of America*, *108*(15), 5954–5963. https://doi.org/10.1073/pnas.1017496108
12. Graham, T. A., Weaver, C., Mao, F., Kimelman, D., & Xu, W. (2000). Crystal Structure of a β-Catenin/Tcf Complex. *Cell*, *103*(6), 885–896. https://doi.org/10.1016/S0092-8674(00)00192-6
13. Hilal, B., Khan, M. M., & Fariduddin, Q. (2024). Recent advancements in deciphering the therapeutic properties of plant secondary metabolites: Phenolics, terpenes, and alkaloids. *Plant Physiology and Biochemistry*, *211*, 108674. https://doi.org/10.1016/j.plaphy.2024.108674
14. Jia, C.-Y., Li, J.-Y., Hao, G.-F., & Yang, G.-F. (2020). A drug-likeness toolbox facilitates ADMET study in drug discovery. *Drug Discovery Today*, *25*(1), 248–258. https://doi.org/10.1016/j.drudis.2019.10.014
15. Johariya, V., Joshi, A., Malviya, N., & Malviya, S. (2023). Introduction to Cancer. In *Medicinal Plants and Cancer Chemoprevention*. CRC Press.
16. Lepourcelet, M., Chen, Y.-N. P., France, D. S., Wang, H., Crews, P., Petersen, F., Bruseo, C., Wood, A. W., & Shivdasani, R. A. (2004). Small-molecule antagonists of the oncogenic Tcf/β-catenin protein complex. *Cancer Cell*, *5*(1), 91–102.

https://doi.org/10.1016/S1535-6108(03)00334-9

17. Liu, J., Xiao, Q., Xiao, J., Niu, C., Li, Y., Zhang, X., Zhou, Z., Shu, G., & Yin, G. (2022). Wnt/β-catenin signalling: Function, biological mechanisms, and therapeutic opportunities. *Signal Transduction and Targeted Therapy*, *7*(1), 3. https://doi.org/10.1038/s41392-021-00762-6
18. Liu, R., Zhang, H., Yuan, M., Zhou, J., Tu, Q., Liu, J.-J., & Wang, J. (2013). Synthesis and Biological Evaluation of Apigenin Derivatives as Antibacterial and Antiproliferative Agents. *Molecules*, *18*(9), Article 9. https://doi.org/10.3390/molecules180911496
19. Liu, S., Zheng, X., Luo, Z., Tang, C., Hu, Y., Peng, Q., Mi, P., Chen, H., & Yao, X. (2024). The synthesis and bioactivity of apigenin derivatives. *Fitoterapia*, *179*, 106228. https://doi.org/10.1016/j.fitote.2024.106228
20. Mannhold, R., Poda, G. I., Ostermann, C., & Tetko, I. V. (2009). Calculation of molecular lipophilicity: State-of-the-art and comparison of log P methods on more than 96,000 compounds. *Journal of Pharmaceutical Sciences*, *98*(3), 861–893. https://doi.org/10.1002/jps.21494
21. Mukherjee, P. K., Nema, N. K., Maity, N., & Sarkar, B. K. (2013). Phytochemical and therapeutic potential of cucumber. *Fitoterapia*, *84*, 227–236. https://doi.org/10.1016/j.fitote.2012.10.003
22. Naponelli, V., Rocchetti, M. T., & Mangieri, D. (2024). Apigenin: Molecular Mechanisms and Therapeutic Potential against Cancer Spreading. *International Journal of Molecular Sciences*, *25*(10), Article 10. https://doi.org/10.3390/ijms25105569
23. Oladeji, S. M., Conteh, D. N., Bello, L. A., Adegboyega, A. E., & Shokunbi, O. S. (2025). Rational Design and Optimization of Novel PDE5 Inhibitors for Targeted Colorectal Cancer Therapy: An In Silico Approach. *International Journal of Molecular Sciences*, *26*(5), Article 5. https://doi.org/10.3390/ijms26051937
24. Pagare, P. P., Morris, A., Li, J., & Zhang, Y. (2021). Development of structure-based pharmacophore to target the β-catenin-TCF protein–protein interaction. *Medicinal Chemistry Research*, *30*(2), 429–439. https://doi.org/10.1007/s00044-020-02693-3
25. Poy, F., Lepourcelet, M., Shivdasani, R. A., & Eck, M. J. (2001). Structure of a human Tcf4–β-catenin complex. *Nature Structural Biology*, *8*(12), 1053–1057. https://doi.org/10.1038/nsb720
26. Roskoski, R. (2023). Rule of five violations among the FDA-approved small molecule protein kinase inhibitors. *Pharmacological Research*, *191*, 106774. https://doi.org/10.1016/j.phrs.2023.106774
27. Samant, C., Kale, R., Pai, K. S. R., Nandakumar, K., & Bhonde, M. (2024). Role of Wnt/β-catenin pathway in cancer drug resistance: Insights into molecular aspects of major solid tumors. *Biochemical and Biophysical Research Communications*, *729*, 150348. https://doi.org/10.1016/j.bbrc.2024.150348
28. Sargsyan, K., Grauffel, C., & Lim, C. (2017). How Molecular Size Impacts RMSD Applications in Molecular Dynamics Simulations. *Journal of Chemical Theory and Computation*, *13*(4), 1518–1524. https://doi.org/10.1021/acs.jctc.7b00028
29. Shang, S., Hua, F., & Hu, Z.-W. (2017). The regulation of β-catenin activity and function in cancer: Therapeutic opportunities. *Oncotarget*, *8*(20), 33972–33989. https://doi.org/10.18632/oncotarget.15687
30. Sherman, W., Beard, H. S., & Farid, R. (2006). Use of an Induced Fit Receptor Structure in Virtual Screening. *Chemical Biology & Drug Design*, *67*(1), 83–84. https://doi.org/10.1111/j.1747-0285.2005.00327.x
31. Sherman, W., Day, T., Jacobson, M. P., Friesner, R. A., & Farid, R. (2006). Novel Procedure for Modeling Ligand/Receptor Induced Fit Effects. *Journal of Medicinal Chemistry*, *49*(2), 534–553. https://doi.org/10.1021/jm050540c
32. Shukla, S., MacLennan, G. T., Flask, C. A., Fu, P., Mishra, A., Resnick, M. I., & Gupta, S. (2007). Blockade of β-Catenin Signaling by Plant Flavonoid Apigenin Suppresses Prostate Carcinogenesis in TRAMP Mice. *Cancer Research*, *67*(14), 6925–6935. https://doi.org/10.1158/0008-5472.CAN-07-0717

33. Sobti, R. C., Thakur, M., & Kaur, T. (2024). Cancer: Epidemiology, Racial, and Geographical Disparities. In R. C. Sobti, H. Sugimura, & A. Sobti (Eds.), *Molecular Biomarkers for Cancer Diagnosis and Therapy* (pp. 31–52). Springer Nature. https://doi.org/10.1007/978-981-99-3746-2_3
34. Søndergaard, C. R., Olsson, M. H. M., Rostkowski, M., & Jensen, J. H. (2011). Improved Treatment of Ligands and Coupling Effects in Empirical Calculation and Rationalization of pKa Values. *Journal of Chemical Theory and Computation*, *7*(7), 2284–2295. https://doi.org/10.1021/ct200133y
35. Tian, W., Han, X., Yan, M., Xu, Y., Duggineni, S., Lin, N., Luo, G., Li, Y. M., Han, X., Huang, Z., & An, J. (2012). Structure-Based Discovery of a Novel Inhibitor Targeting the β-Catenin/Tcf4 Interaction. *Biochemistry*, *51*(2), 724–731. https://doi.org/10.1021/bi201428h
36. Trosset, J.-Y., Dalvit, C., Knapp, S., Fasolini, M., Veronesi, M., Mantegani, S., Gianellini, L. M., Catana, C., Sundström, M., Stouten, P. F. W., & Moll, J. K. (2006). Inhibition of protein–protein interactions: The discovery of druglike β-catenin inhibitors by combining virtual and biophysical screening. *Proteins: Structure, Function, and Bioinformatics*, *64*(1), 60–67. https://doi.org/10.1002/prot.20955
37. Tuama, A. A., & Mohammed, A. A. (2019). Phytochemical screening and in vitro antibacterial and anticancer activities of the aqueous extract of *Cucumis sativus*. *Saudi Journal of Biological Sciences*, *26*(3), 600–604. https://doi.org/10.1016/j.sjbs.2018.07.012
38. van de Waterbeemd, H., & Gifford, E. (2003). ADMET in silico modelling: Towards prediction paradise? *Nature Reviews Drug Discovery*, *2*(3), 192–204. https://doi.org/10.1038/nrd1032
39. Voronkov, A., & Krauss, S. (2013). Wnt/beta-Catenin Signaling and Small Molecule Inhibitors. *Current Pharmaceutical Design*, *19*(4), 634–664. https://doi.org/10.2174/138161213804581837
40. Wang, K., Qiu, X., Zhao, Y., Wang, H., & Chen, L. (2022). The Wnt/β-catenin signaling pathway in the tumor microenvironment of hepatocellular carcinoma. *Cancer Biology & Medicine*, *19*(3), 305–318. https://doi.org/10.20892/j.issn.2095-3941.2021.0306
41. Xu, M., Wang, S., Song, Y., Yao, J., Huang, K., & Zhu, X. (2016). Apigenin suppresses colorectal cancer cell proliferation, migration and invasion via inhibition of the Wnt/β-catenin signaling pathway. *Oncology Letters*, *11*(5), 3075–3080. https://doi.org/10.3892/ol.2016.4331
42. Yan, M., Li, G., & An, J. (2017). Discovery of small molecule inhibitors of the Wnt/β-catenin signaling pathway by targeting β-catenin/Tcf4 interactions. *Experimental Biology and Medicine*, *242*(11), 1185–1197. https://doi.org/10.1177/1535370217708198
43. Yan, X., Qi, M., Li, P., Zhan, Y., & Shao, H. (2017). Apigenin in cancer therapy: Anti-cancer effects and mechanisms of action. *Cell & Bioscience*, *7*(1), 50. https://doi.org/10.1186/s13578-017-0179-x
44. Yu, B., Huang, Z., Zhang, M., Dillard, D. R., & Ji, H. (2013). Rational Design of Small-Molecule Inhibitors for β-Catenin/T-Cell Factor Protein–Protein Interactions by Bioisostere Replacement. *ACS Chemical Biology*, *8*(3), 524–529. https://doi.org/10.1021/cb300564v
45. Zhang, H., Zhao, H., Chi, M., Yang, K., Chen, Y., Mao, J., Li, P., Wang, Z., Song, F., Guo, W., Sakai, M., Takahashi, J., Zhang, H., Zhao, H., Chi, M., Yang, K., Chen, Y., Mao, J., Li, P., … Takahashi, J. (2023). A systematic review on the development of radiosensitizers, with cancer selectivity, for radiotherapy using ionizing radiation. *AIMS Bioengineering*, *10*(2), Article bioeng-10-02-008. https://doi.org/10.3934/bioeng.2023008
46. Zhang, Y., & Wang, X. (2020). Targeting the Wnt/β-catenin signaling pathway in cancer. *Journal of Hematology & Oncology*, *13*(1), 165. https://doi.org/10.1186/s13045-020-00990-3
47. Zhao, H., Ming, T., Tang, S., Ren, S., Yang, H., Liu, M., Tao, Q., & Xu, H. (2022). Wnt signaling in colorectal cancer: Pathogenic role and therapeutic target. *Molecular Cancer*, *21*(1), 144. https://doi.org/10.1186/s12943-022-01616-7
48. Zhao, M., Chen, Y., & Yang, L.-H. (2024). Advancements in the study of glucose metabolism in relation to tumor progression and treatment. *Progress in Biophysics and Molecular Biology*, *192*, 11–18.

https://doi.org/10.1016/j.pbiomolbio.2024.08.001

49. Zhou, X., Wang, F., Zhou, R., Song, X., & Xie, M. (2017). Apigenin: A current review on its beneficial biological activities. *Journal of Food Biochemistry*, *41*(4), e12376. https://doi.org/10.1111/jfbc.12376

Figures

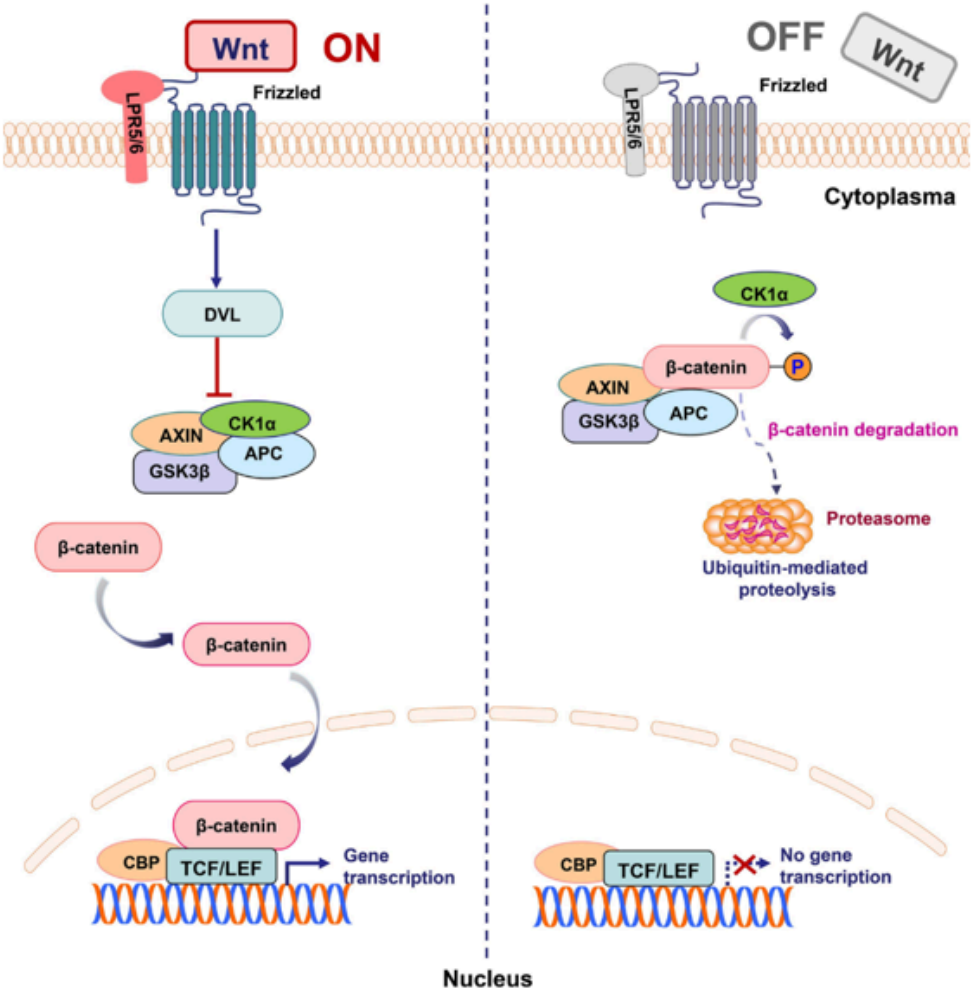


Figure 1

Wnt/β-catenin pathway (Y. Zhang & Wang, 2020).



Figure 2

Cucumber

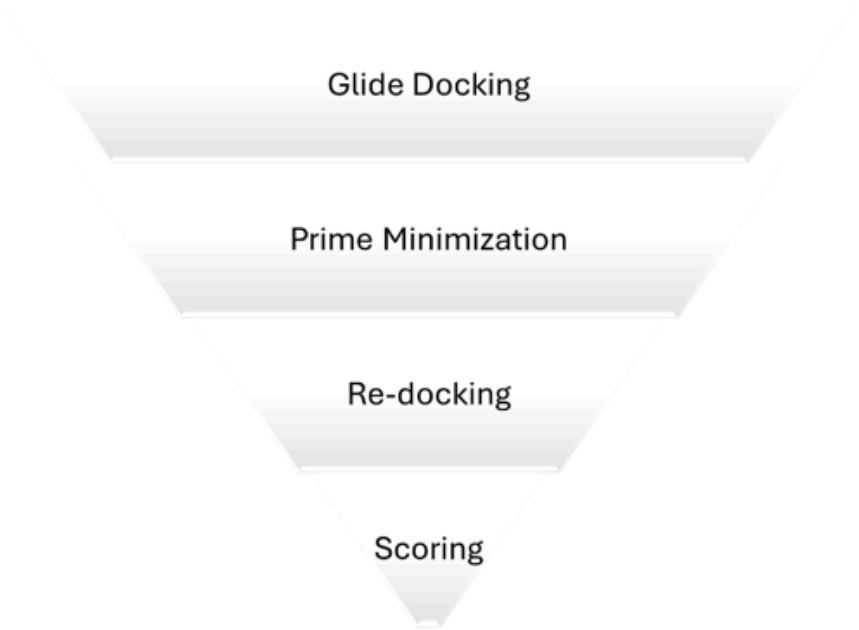
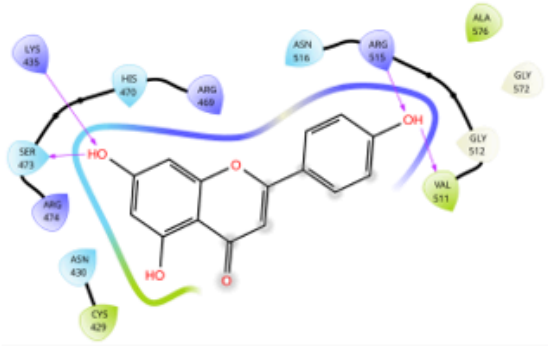
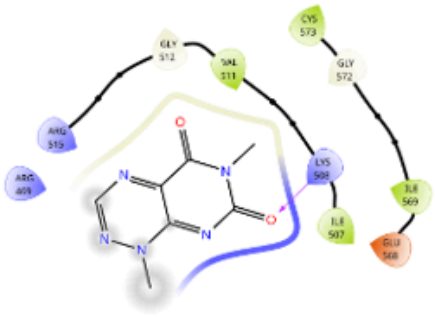


Figure 3

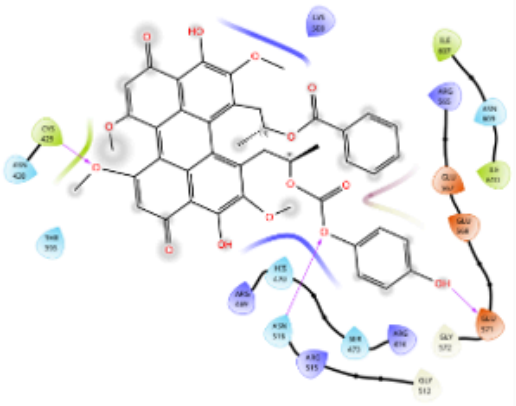
IFD docking protocol



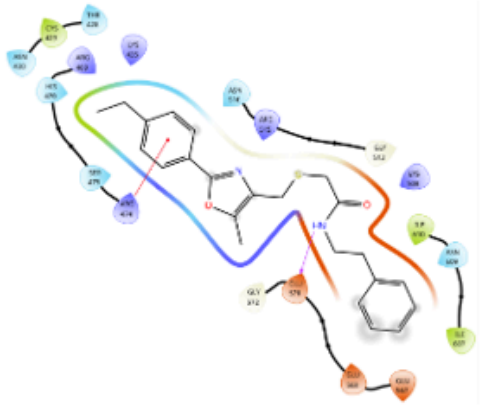
Apigenin



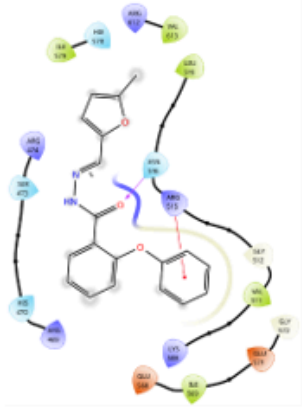
PKF118-310



PKF115-584



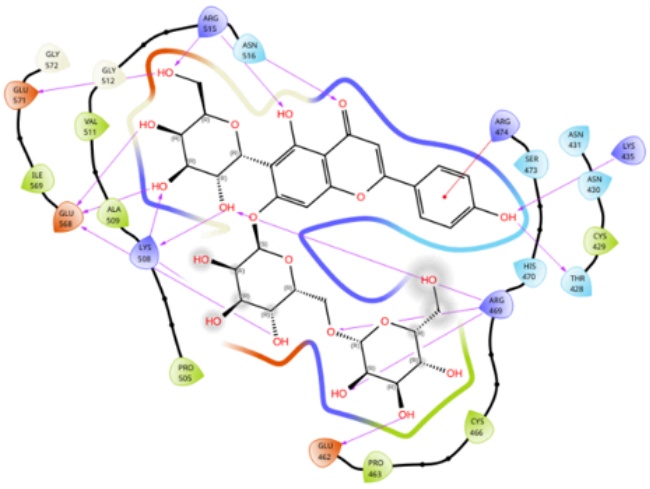
iCRT3



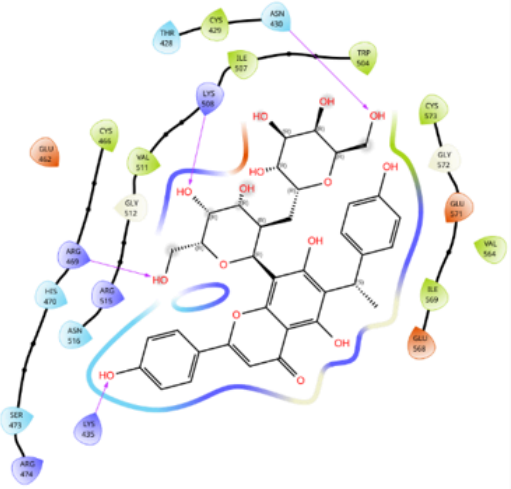
PNU-74654

Figure 4

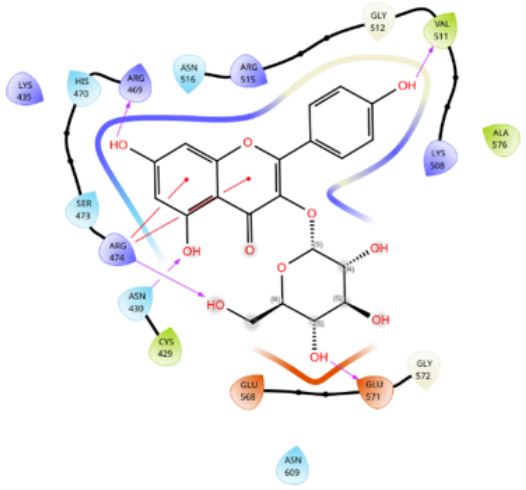
2D molecular interactions of β-catenin with top 4 standard ligands (Apigenin, PKF118-310, PKF115-584, iCRT3) and PNU-74654.



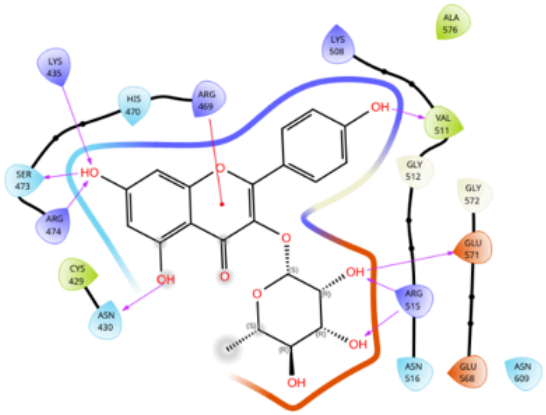
Isovitexin-7-O-(6-O-glucosyl)-glucoside



Cucumerin C



Kaempferol 3-O-glucoside



Kaempferol 3-O-rhamnoside

Figure 5

2D molecular interactions of β-catenin with top 4 phytochemical ligands, Isovitexin-7-O-(6-O-glucosyl)-glucoside, Cucumerin C, Kaempferol 3-O-glucoside, and Kaempferol 3-O-rhamnoside.

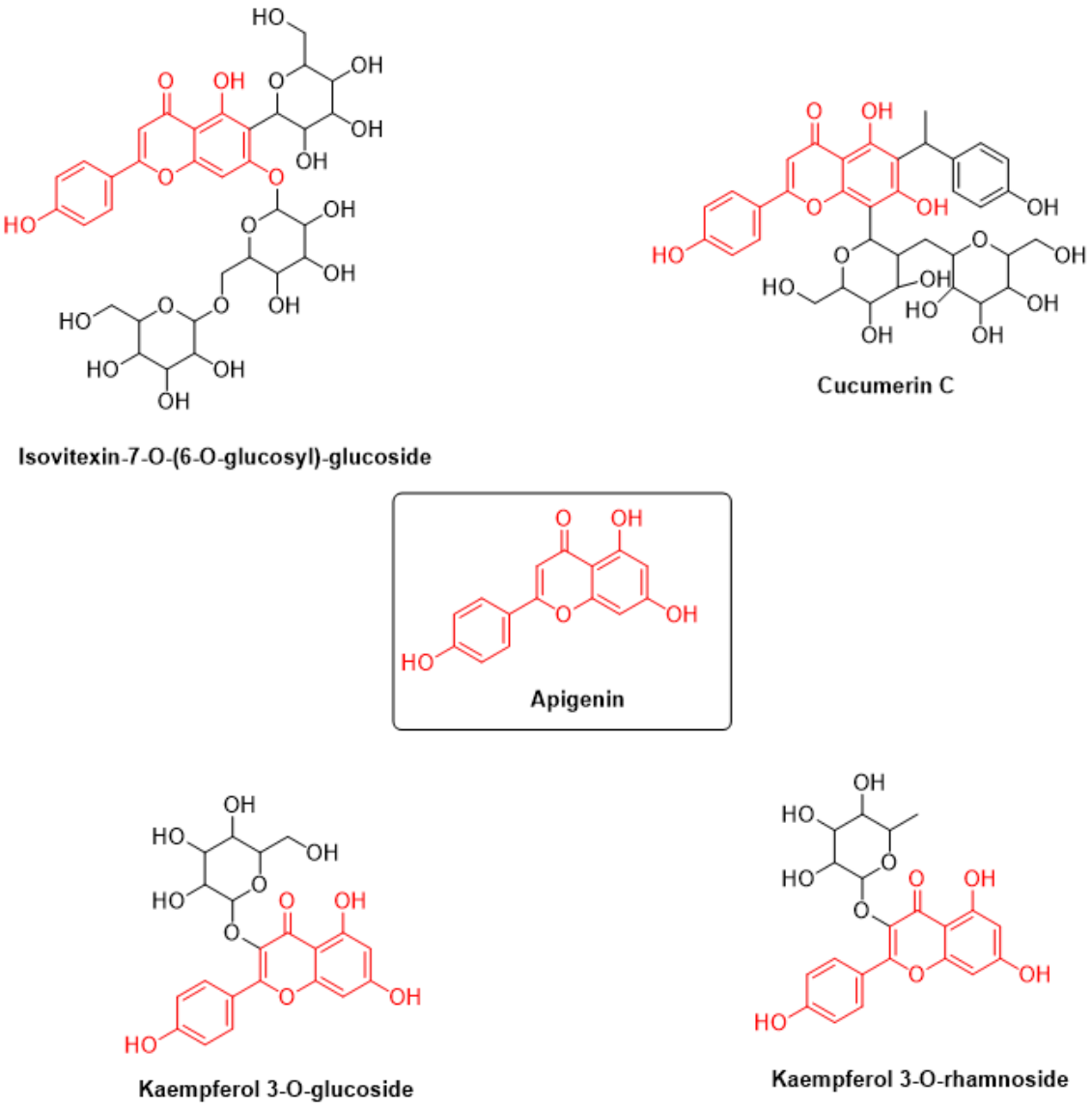


Figure 6

Structures of the top four ligands, Isovitexin-7-O-(6-O-glucosyl)-glucoside, Cucumerin C, Kaempferol 3-O-glucoside, and Kaempferol 3-O-rhamnoside, showing the Apigenin common core structure.

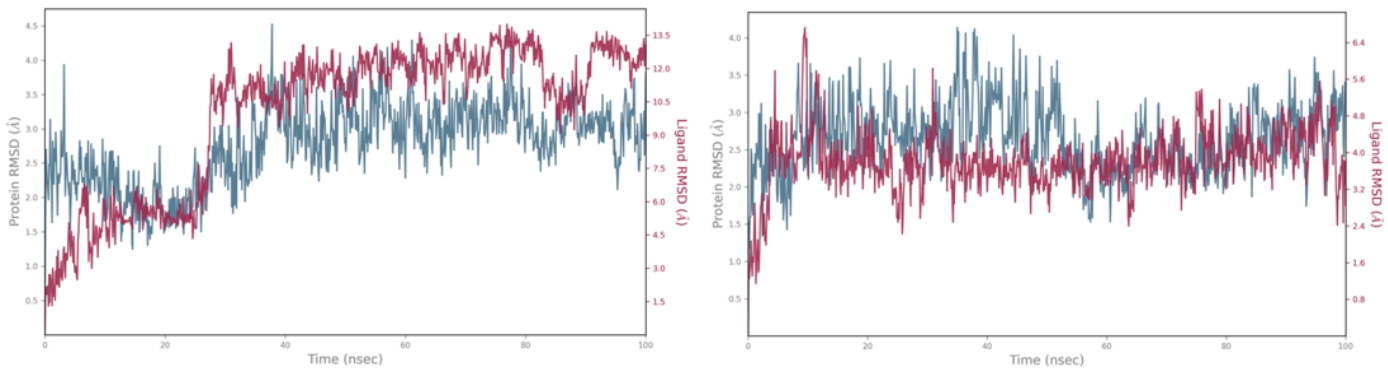


Figure 7

RMSD plots of β-catenin complexes with Isovitexin-7-O-(6-O-glucosyl)-glucoside (left) and Cucumerin C (right).

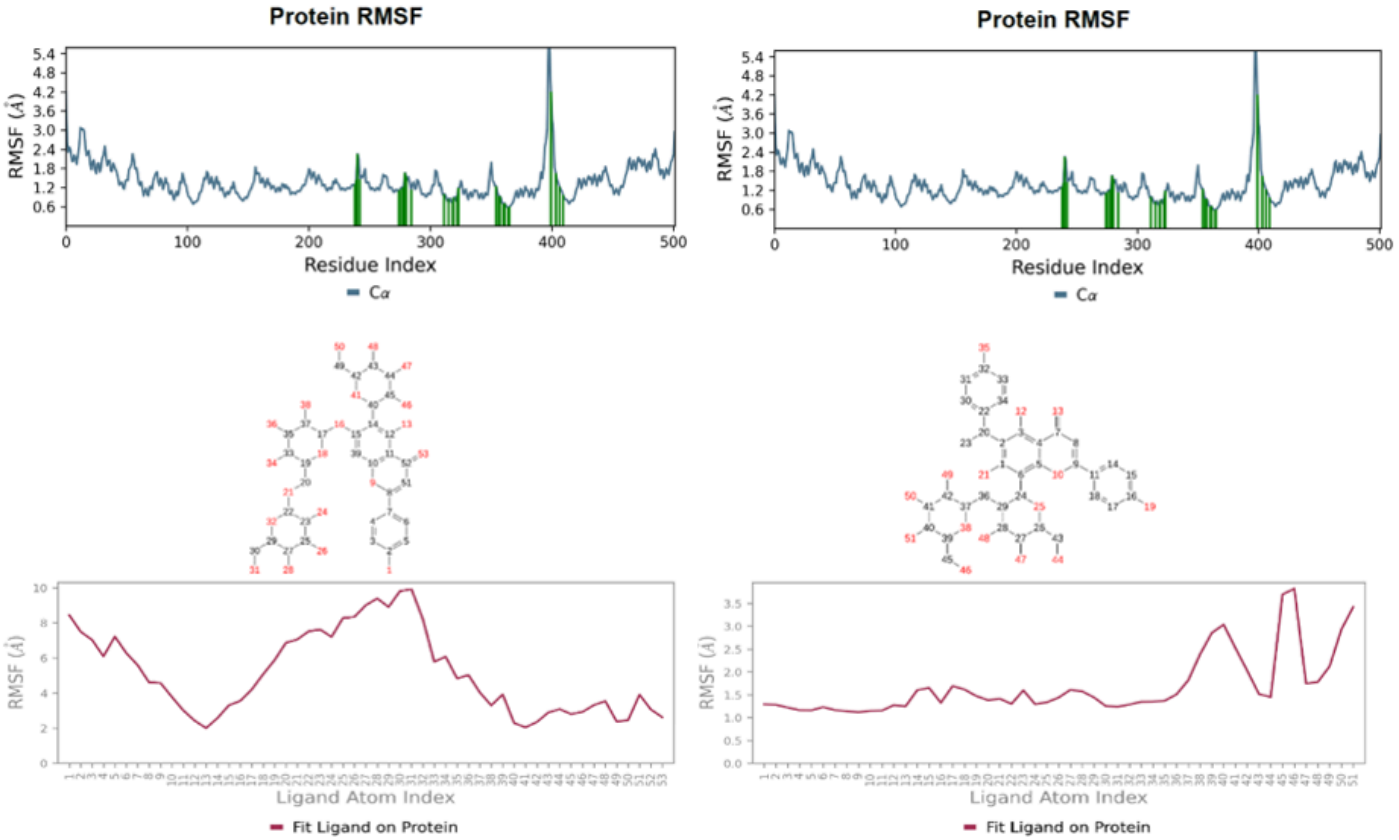


Figure 8

Protein (top) and ligand (bottom) root mean square flunctuations of Isovitexin-7-O-(6-O-glucosyl)-glucoside (left) and Cucumerin C (right).

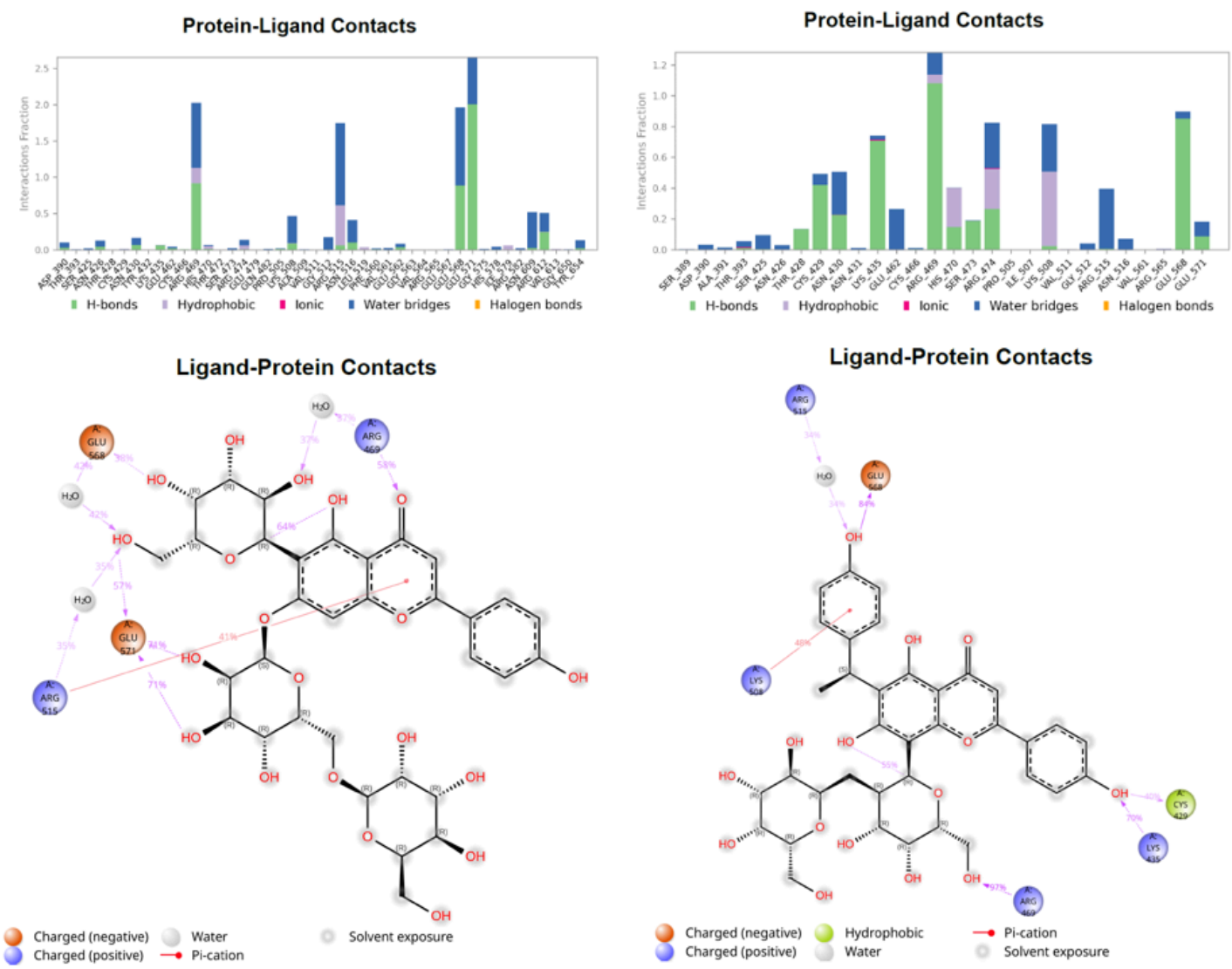


Figure 9

Protein–Ligand Contacts (top) and Ligand–Protein Contacts (bottom) plots illustrating the binding interactions between the protein and Isovitexin-7-O-(6-O-glucosyl)-glucoside (left), and Cucumerin C (right).